Journal of Medicinal Chemistry Article

J. Med. Chem. **2009,** *52,* 7593–7603 **7593**
DOI: 10.1021/jm900433t

Crystallographic Snapshots of Nonaged and Aged Conjugates of Soman with Acetylcholinesterase, and of a Ternary Complex of the Aged Conjugate with Pralidoxime[†,‡]

Benoît Sanson,[§] Florian Nachon,[∥] Jacques-Philippe Colletier,[§] Marie-Thérèse Froment,[∥] Lilly Toker,[#] Harry M. Greenblatt,[⊥] Joel L. Sussman,[⊥] Yaacov Ashani,[#] Patrick Masson,[∥,§] Israel Silman,[#] and Martin Weik*[,§]

[§]*Laboratoire de Biophysique Moléculaire, Institut de Biologie Structurale Jean-Pierre Ebel, Commissariat à l'Énergie Atomique, Centre National de la Recherche Scientifique, Université Joseph Fourier, 41 Rue Jules Horowitz, 38027 Grenoble, France,* [∥]*Département de Toxicologie, Centre de Recherches du Service de Santé des Armées, 24 Avenue des Maquis du Grésivaudan, 38700 La Tronche, France,* [⊥]*Department of Structural Biology and* [#]*Department of Neurobiology, Weizmann Institute of Science, Rehovot 76100, Israel*

Received April 3, 2009

Organophosphate compounds (OP) are potent inhibitors of acetylcholinesterases (AChEs) and can cause lethal poisoning in humans. Inhibition of AChEs by the OP soman involves phosphonylation of the catalytic serine, and subsequent dealkylation produces a form known as the "aged" enzyme. The nonaged form can be reactivated to a certain extent by nucleophiles, such as pralidoxime (2-PAM), whereas aged forms of OP-inhibited AChEs are totally resistant to reactivation. Here, we solved the X-ray crystal structures of AChE from *Torpedo californica* (*Tc*AChE) conjugated with soman before and after aging. The absolute configuration of the soman stereoisomer adduct in the nonaged conjugate is P_SC_R. A structural reorientation of the catalytic His440 side chain was observed during the aging process. Furthermore, the crystal structure of the ternary complex of the aged conjugate with 2-PAM revealed that the orientation of the oxime function does not permit nucleophilic attack on the phosphorus atom, thus providing a plausible explanation for its failure to reactivate the aged soman/AChE conjugate. Together, these three crystal structures provide an experimental basis for the design of new reactivators.

Introduction

The principal role of acetylcholinesterase (AChE,[a] EC 3.1.1.7) is termination of nerve impulse transmission at cholinergic synapses by rapid hydrolysis of the neurotransmitter acetylcholine (ACh).[1] In keeping with its biological role, AChE is a very rapid enzyme, with a turnover number of 10^3-10^4 s^{-1}, depending on the species. The first X-ray structure of an AChE, that from *Torpedo californica* (*Tc*AChE), revealed that its active site is buried at the bottom of a deep and narrow gorge.[2] It features a catalytic triad (Ser200, His440, Glu327), typical of serine hydrolases, and a catalytic anionic subsite (CAS), in which the choline moiety of ACh is stabilized via cation$-\pi$ interactions with Trp84 and Phe330 and by an electrostatic interaction with Glu199.[2,3] Stabilization of ACh in the active site also involves interactions of its carbonyl oxygen within the oxyanion hole (Gly118, Gly119, Ala201) and of the methyl moiety of its acetyl group in the acyl pocket (Trp233, Phe288, Phe290, Phe331).[4] At the rim of the gorge, Trp279 is the main component of a so-called "peripheral" anionic site (PAS) that interacts allosterically with the active site[5] and mediates trapping of the substrate en route to the active site.[3,6]

AChE is the target of numerous inhibitors, both covalent (irreversible) and noncovalent (reversible), including most approved anti-Alzheimer drugs, and neurotoxins such as the fasciculins, carbamates, and organophosphates (OPs).[1] OPs include both insecticides and chemical warfare agents that lead to irreversible inhibition of AChE. Intoxication by OP-based insecticides is a serious public health problem, causing the death of some 200000 people per year throughout the world.[7] The lethality of OP nerve agents was evident both when they were employed by Iraqi troops against Iranian troops and Kurd civilians in 1988[8−11] and in the Tokyo subway terrorist attack in 1995.[12] Detailed understanding of the mechanism of AChE inhibition by OPs is thus of major importance in a toxicological context, inasmuch as it may provide crucial information for the rational design of new antidotes.

Soman, *O*-(1,2,2-trimethylpropyl) methylphosphonofluoridate, is one of the most toxic OPs. Inhibition of AChE by soman involves covalent modification of Ser200 (*Tc*AChE residue numbering throughout the manuscript unless stated otherwise), by a mechanism that implicates nucleophilic attack of the latter on the phosphorus atom of soman, with concomitant departure of its fluoride atom (Scheme 1).

[†] We acknowledge the 100th anniversary of the Division of Medicinal Chemistry of the American Chemical Society.

[‡] The atomic coordinates and structure factors (codes 2wfz, 2wg0, and 2wg1) have been deposited in the RCSB Protein Data Bank, www.rcsb.org.

*To whom correspondence should be addressed. Phone: (33) 4 38 78 95 69. Fax: (33) 4 38 78 54 94. E-mail: weik@ibs.fr.

[a] Abbreviations: AChE, acetylcholinesterase; OP, organophosphate; *Tc*, *Torpedo californica*; 2-PAM, pralidoxime, *N*-methylpyridin-1-ium 2-aldoxime methiodide; ACh, acetylcholine; CAS, catalytic anionic subsite; PAS, peripheral anionic site; BChE, butyrylcholinesterase; TMB-4, trimedoxime bromide; CE1, carboxylesterase 1; PEG, polyethyleneglycol; MES, morpholinoethylsulphonic acid; NAG, *N*-acetylglucosamine; FUC, fucose.

Published on Web 07/30/2009

Scheme 1. Irreversible Iinhibition of AChE by Soman (Upper Panel) and Reactivation of the Nonaged Enzyme with 2-PAM (Lower Panel)[a]

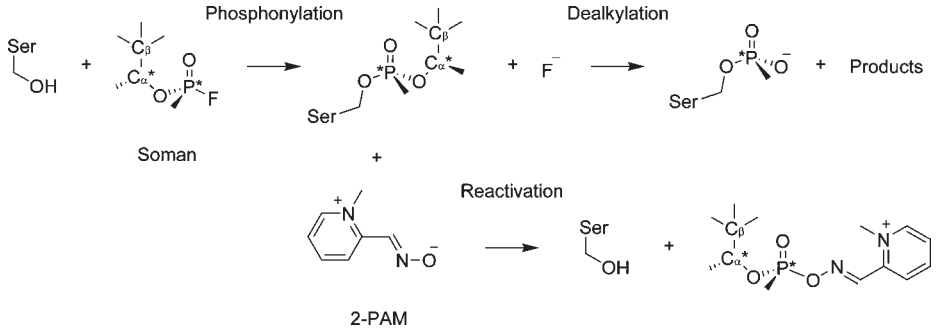

[a] The catalytic Ser200 first performs a nucleophilic attack on the phosphorous atom. Then the enzyme catalyzes departure of the pinacolyl group (dealkylation or "aging"). Prior to "aging", reactivation of AChE can occur via nucleophilic attack of the oxime group of 2-PAM on the phosphorus atom of the phosphonyl adduct, resulting in its cleavage from Ser 200 Oγ. Asterisks denote chiral centers.

Subsequently, AChE catalyzes the dealkylation of the OP adduct at a rate ca. 10^{10} higher than that at which non-enzymatic dealkylation would occur.[13] This second step has been termed "aging" and transforms the nonaged soman/AChE conjugate into an aged conjugate that can no longer be rescued by the available reactivators.[14] Among all OPs known to date, with the exception of CH_3POF_2 and CH_3POCl_2,[15,16] soman is the one that produces an aged enzyme most rapidly. Extrapolated half-lives of aging of soman/AChE conjugates range from seconds to several minutes under near physiological conditions.[13,17−19] For the soman/*Tc*AChE conjugate, half-lives for aging of 1.9 and 3.9 min were reported at pH 6.5 and 7.5, respectively, at room temperature.[17]

The mechanism of enzyme-induced aging is not fully understood, and the chemical basis for the unusually fast rate of dealkylation of soman/AChE conjugates requires further clarification. Two pathways were considered in which either protonation of the pinacolyl oxygen[14,19] or methyl migration from Cβ to Cα of the pinacolyl group[13,17,20] were proposed to be rate-determining. Regardless of the mechanistic details, it is agreed that dealkylation is accompanied by O−C scission of the P−O−$CH(CH_3)C(CH_3)_3$ chain (Scheme 1) and that Glu199, Phe331, Glu443, His440, and in particular, Trp84, play important roles in the aging process.[13,17,19,20] It is of interest that the aged soman/AChE conjugate is analogous to the deacylation tetrahedral intermediate of acetylated AChE.[21−23]

Soman contains two chiral centers, the P and Cα atoms, and thus occurs as four stereoisomers. AChEs react preferentially with the P_S enantiomers, with phosphylation rates $\sim 5 \times 10^4$ higher for the P_S than for the P_R enantiomers.[24,25] An in-line displacement of fluoride by Ser200 has been proposed,[26] implying that the stereochemistry of the phosphorus atom is reversed following conjugation to the enzyme. The P_R configuration in the crystal structure of the nonaged phosphonylated *Tc*AChE conjugate obtained by use of the *O*-ethyl methylphosphonyl OP, VX, is indeed consistent with inversion at the P atom.[27] As for the preference of AChE for the configuration at the Cα atom, the rates of inhibition of human (hu) AChE,[25] bovine AChE,[28] eel AChE,[28] equine butyrylcholinesterase (BChE ; EC 3.1.1.8),[25] and huBChE[18,29] by the P_SC_S stereoisomer are consistently (though only slightly) higher than by the P_SC_R stereoisomer.

Oximes are capable of reactivating nonaged OP/AChE conjugates[30,31] by nucleophilic attack of the oxime group ($R_1R_2C{=}NOH$) on the phosphorus atom.[32,33] So far, only a few oximes have been included in therapeutic regimens for treatment of OP intoxication, viz. *N*-methylpyridin-1-ium 2-aldoxime methiodide (pralidoxime, 2-PAM), trimedoxime bromide (TMB-4), and toxogonin.[34] The bis-quaternary oximes, HI-6 and HLö-7, have, so far, been the most effective in reactivation of most nonaged OP/huAChE conjugates.[35] The nonaged soman/huAChE conjugate obtained by use of the P_SC_S isomer has been reported to be significantly more amenable to reactivation by HI-6 than the P_SC_R adduct.[36] Although great efforts are being made to produce more potent reactivators,[37] no single broad-spectrum reactivator has, so far, been described that is capable of reactivating all nonaged nerve agent/AChE conjugates.[38] Furthermore, it has been observed that phosphonylated oximes, which are formed during reactivation, are capable of reinhibiting AChE.[39,40]

The X-ray structures of several nonaged and aged OP/AChE conjugates have been solved in recent years. Those of the nonaged VX/*Tc*AChE conjugate[27] and of the nonaged tabun conjugate of murine AChE[41] (mAChE) both showed that a reorientation of the side chain of the catalytic histidine is necessary to accommodate the ethoxy group common to the two inhibitors. Upon aging, these structural changes are reversed and the catalytic histidine in the aged OP/AChE conjugate reverts to its native conformation. The structure of the aged soman/*Tc*AChE was determined by crystallizing the inhibited enzyme, and here, too, the side chain of the catalytic His residue was seen to be in its native orientation.[23] However, due to the experimental difficulties imposed by the rapidity of the aging process, the crystal structure of the nonaged soman/AChE conjugate had not been reported.

Here, we present the crystal structures of nonaged and in crystallo aged soman/*Tc*AChE conjugates and of a ternary complex of the aged conjugate with the oxime reactivator, 2-PAM. These structures provide important information that can be utilized in clarifying: (a) the influence of the architecture of the catalytic site and of water molecules within the gorge on the rate and mechanism of the aging reaction and (b) the resistance of aged OP-AChE conjugates to reactivation. Hopefully, such clarifications will facilitate the quest for new reactivators of OP-inhibited AChE.

Results

Nonaged Soman/TcAChE Conjugate. Trapping of the nonaged soman/*Tc*AChE was achieved by reducing the

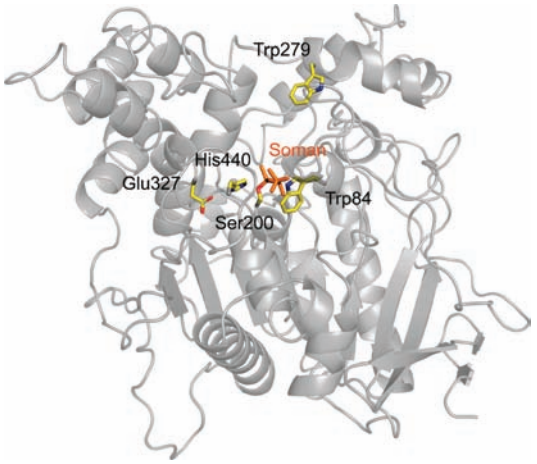

Figure 1. Overall view of the nonaged soman/*Tc*AChE conjugate. The backbone of the enzyme is displayed as a gray ribbon, with the entrance to the active-site gorge at the top. The catalytic triad residues (Ser200, His440, and Glu327), as well as the main residues of the CAS and PAS, Trp84, and Trp279, respectively, are represented as yellow sticks and the OP moiety as orange sticks.

soaking time to 6 min and raising the pH to 8.2, a pH value at which aging is significantly retarded.[13,14]

The structure, solved at 1.95 Å resolution, is displayed in Figure 1. The initial $F_o - F_c$ electron density map featured a 12σ peak at covalent bonding distance from Ser200 Oγ, clearly revealing the position of the phosphorus atom of the phosphonyl group. At lower σ levels, the pinacolyl group is clearly defined (Figure 2A). It is stabilized by hydrophobic interaction with Trp84; thus, one of the methyl groups of the pinacolyl Cβ atom (Scheme 1) is 3.6 Å from the nearest nonhydrogen atom of Trp84.

The catalytic His440 is H-bonded to both Ser200 Oγ (2.7 Å) and Glu327 Oε1 (2.6 Å) through its Nε2 and Nδ1 nitrogens, respectively. The soman O2 atom is within H-bonding distance (3.2 Å) of His440 Nε2, although the bond angle is unfavorable. Thus, the proton on His440 Nε2 is preferentially oriented toward Ser200 Oγ (Nε2−H−Oγ angle 142°, H−Oγ distance 1.8 Å), rather than toward soman O2 (Nε2−H−O2 angle 118°, H−O2 distance 2.6 Å). Mimicking the carbonyl oxygen of the natural substrate, ACh, soman O1 establishes three H-bonds within the oxyanion hole with Gly118 N (2.7 Å), Gly119 N (2.6 Å), and Ala201 N (3.0 Å; not shown in Figure 2A). Noteworthy, also, is a weak H-bond between soman O2 and water 1001, located up the gorge (3.3 Å), which is also within H-bonding distance (3.3 Å) of Tyr121 Oζ. Glu199 Oε1 is 3.1 Å from the methyl group on the Cα atom and 4.0 Å from the closest methyl group on the Cβ atom of soman (not shown). Glu199 itself is stabilized by Glu443 through hydrogen bonds with the bridging water 1002, just as was observed for native *Tc*AChE.[2,42]

The pinacolyl moiety in the nonaged conjugate perturbs the position of the imidazole ring of His440; consequently, its Nε2 nitrogen is shifted by 0.5 Å relative to its position in the native structure. This is in contrast to the total disruption of the catalytic triad observed in the nonaged VX/*Tc*AChE conjugate.[27] Several other residues in the vicinity of the active site are slightly affected by phosphonylation of Ser200. These include Trp84, Trp233, Phe330, Tyr334, and Tyr442, all located in the bottom half of the gorge. Their movements result in a small (6%) decrease in the volume of the active-site gorge relative to native *Tc*AChE.

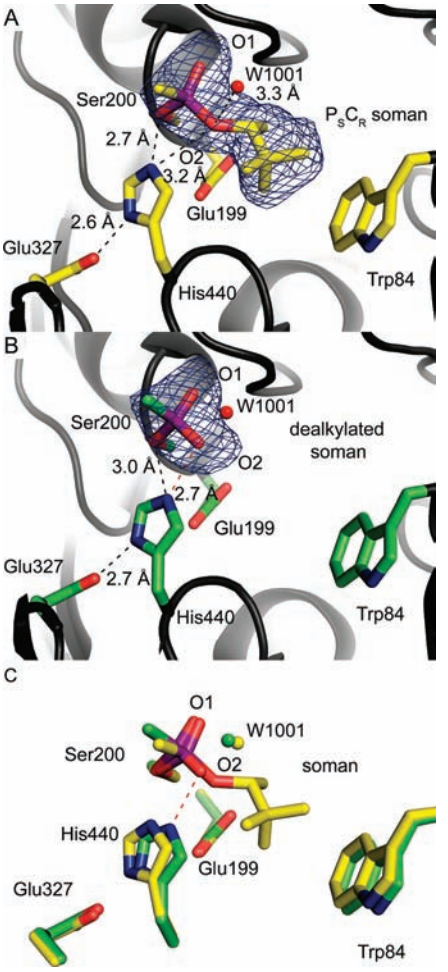

Figure 2. Active sites of the nonaged (A) and aged (B) soman/*Tc*AChE conjugates and their superposition (C). The $F_o - F_c$ omit maps are contoured at 3σ. The catalytic triad residues (Ser200, His440, and Glu327), Trp84, and the OP adducts are displayed as sticks, with oxygen atoms in red, nitrogen atoms in blue, and the phosphorus atom in purple. Carbon atoms of the nonaged conjugate are shown in yellow and those of the aged conjugate in green. A water molecule (1001) interacting with soman O2 is represented as a red ball in (A) and (B), and as yellow and green balls in the nonaged and aged structures, respectively, in (C). Hydrogen bonds and a salt bridge are represented as black and red dashed lines, respectively. The apical nitrogen atom of His440 forms a salt bridge (dashed line) with the negatively charged O2 atom of the soman adduct in the aged conjugate.

The soman soaked into the crystals was a mixture of the four stereoisomers, $P_{R/S}C_{R/S}$. As mentioned above,[23] in aqueous solution, AChE reacts preferentially with the P_S enantiomers of soman (Figure 2A). The crystal structure permits assignment of the absolute configuration of the phosphorus atom as P_S and the fact that the pinacolyl group is retained in the nonaged conjugate permits assignment of the absolute configuration of the Cα carbon to be C_R. It should be noted that the methyl group on the Cα carbon hinders its direct interaction with the carboxyl group of Glu199 (distance Cα−Oε1 4.2 Å; Figure 2A).

Aged Soman/TcAChE Conjugate. To favor the dealkylation reaction,[13,14] the pH of the soaking solution was decreased relative to that used to obtain the nonaged conjugate and the time of soaking was increased. The structure of the aged conjugate was solved at 2.2 Å resolution (Figure 2B). No electron density is observed for the pinacolyl group,

demonstrating that the in crystallo dealkylation of soman, viz., aging of the conjugate, had indeed occurred. The phosphorus atom adopts a tetrahedral conformation, being linked to Ser200 Oγ, to the methyl carbon, and to the two oxygens. As observed in the nonaged conjugate, the O1 atom of the phosphonyl moiety is stabilized by H-bonds with the three components of the oxyanion hole, viz. Gly118 N (2.7 Å), Gly119 N (2.6 Å), and Ala201 N (2.8 Å; not shown in Figure 2B). The negatively charged O2 atom points toward Trp84 and establishes a salt bridge[43,44] with His440 Nε2 (2.7 Å). This interaction distance value is in agreement with that reported by Shafferman et al. (2.8 Å)[19] and with that previously observed in the crystal structure of the aged soman/*Tc*AChE conjugate (2.6 Å).[23] His440 is also hydrogen-bonded to Ser200 Oγ through its Nε2 nitrogen (3.0 Å) and to Glu327 through its Nδ1 nitrogen (2.7 Å). The methyl group of the phosphonyl moiety points toward the acyl pocket (distance of 3.6 Å between closest non-hydrogen atoms). The limited conformational changes reduce the volume of the gorge by 3% compared to the volume of the gorge of the native enzyme.

No significant difference was observed between our crystal structure and that reported earlier after crystallization of the aged conjugate,[23] showing that aging in solution and in crystallo produce the same final state.

Superposition of the structures of the nonaged and aged conjugates reveals a small, yet crucial, movement within the active site (Figure 2C): the imidazole ring of His440 is tilted back (Nε2 shifts by 0.8 Å) to a native-like conformation after aging. The resulting proximity between soman O2, which is negatively charged, and His440 Nε2, results in formation of a salt bridge (2.7 Å) (Figure 2B). It should be noted that water molecule 1001, which interacts with soman O2 in the non-aged crystal structure (Figure 2A), is not within H-bonding distance (3.7 Å) of O2 in the aged crystal structure (Figure 2B).

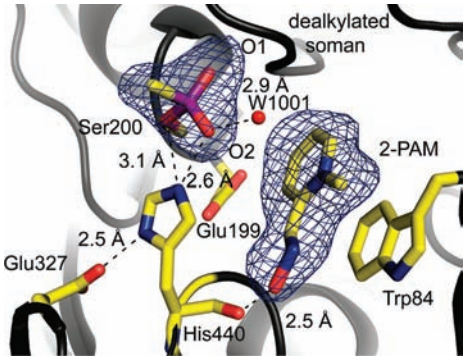

Figure 3. Ternary complex of 2-PAM with the aged soman/*Tc*AChE conjugate. The $F_o - F_c$ omit map is contoured at 3σ. The catalytic triad residues (Ser200, His440, and Glu327) and Trp84 are represented as sticks, and color-coding of these residues, of the OP adduct and of 2-PAM, are as in Figure 2A. A water molecule (1001) interacting with O2 of soman and with the nitrogen atom of 2-PAM is represented as a red ball. Hydrogen bonds are shown as dashed lines.

Ternary Complex of 2-PAM with the Aged Soman/*Tc*AChE Conjugate. The structure of the ternary complex of the aged conjugate with the oxime reactivator, 2-PAM, was solved at 2.2 Å resolution. A molecule of 2-PAM is seen at the CAS but not at the PAS. 2-PAM interacts via parallel π-stacking with the indole moiety of Trp84 (distance of 3.5 Å between closest non-hydrogen atoms) (Figure 3). The oxime oxygen is 2.5 Å from His440 O. The conformation of the phosphonyl adduct on Ser200 is not affected by the presence of 2-PAM, and the oxime oxygen is 6.8 Å from the phosphorus atom. This distance precludes nucleophilic attack at the soman phosphorus atom by the oxime, which would be essential for displacing it from Ser200 Oγ. Water molecule 1001 (Figure 3) bridges 2-PAM and the phosphonyl adduct; it is H-bonded to soman O2 (2.8 Å) and interacts electrostatically with 2-PAM N1 (3.4 Å). Noteworthy is the rotation of Phe330 χ1 and χ2 angles, both by ~50°, which brings the residue across the gorge. It should be noted that a PEG molecule spans the gorge (not shown) from the vicinity of Tyr70/Trp279 down to residues Tyr334/Phe330/Phe331, in the middle of the gorge; yet it does not interact with 2-PAM (distance of 5.9 Å between closest non-hydrogen atoms). The crystal structure presented was solved after soaking crystals of the aged conjugate with 2-PAM at pH 5.6. A structure solved after soaking in 2-PAM at pH 8.2 reproduced all the structural details shown in Figure 3 (data not shown). Thus, the ionization state of the oxime group in solution (pK_a = 7.8)[45] does not appear to influence the mode of 2-PAM binding, which is likely to be governed principally by the hydrophobic interaction with Trp84.

Discussion

This study presents, for the first time, the crystal structure of a nonaged soman/AChE conjugate that was obtained by rapid flash-cooling of crystals of *Tc*AChE soaked with soman at high pH and low temperature, so as to preclude significant aging. The corresponding aged conjugate was generated in crystallo by a longer incubation of the soman-soaked crystals at a lower pH. The aged conjugate was further used to obtain a tertiary complex with the oxime reactivator, 2-PAM. These structures provide valuable information for understanding: (a) the molecular details of the rapid phosphonylation of AChE by soman and of the aging process and (b) the resistance of the aged enzyme to the theoretically possible

Scheme 2. Phosphylation Reaction Scheme of AChE with Either Soman (Upper Panel) or VX (Lower Panel)

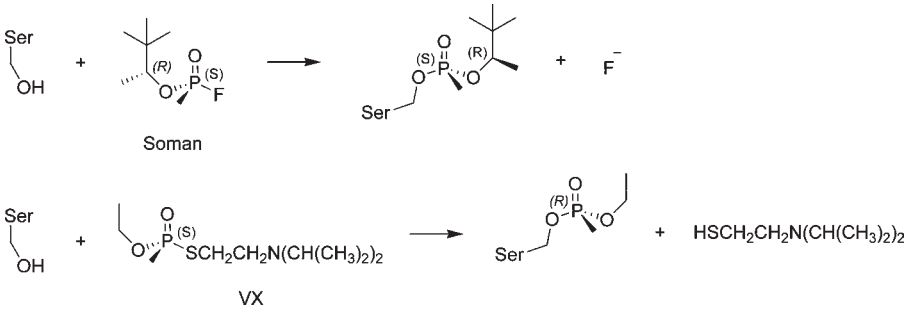

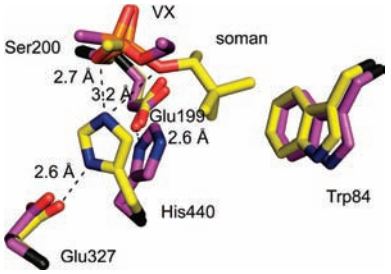

Figure 4. Superposition of the active sites of the nonaged soman/*Tc*AChE and nonaged VX/*Tc*AChE conjugates. Carbon atoms of the soman/*Tc*AChE conjugate are shown in yellow, and those of the VX/*Tc*AChE conjugate in purple. Oxygen and nitrogen atoms are in red and blue, respectively, for the two structures, and phosphorus atoms in orange. Hydrogen bonds are represented as dashed lines.

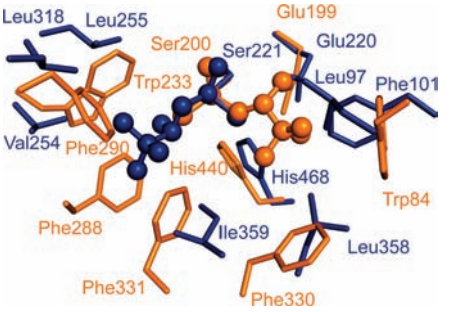

Figure 5. Superposition of the active sites of nonaged soman/*Tc*AChE (orange) and soman/huCE1 (blue) conjugates. The residues and the OP moieties are represented as ball-and-stick models. Labels for *Tc*AChE and huCE1 residues are in orange and blue, respectively.

reactivation. These, in turn, may provide a basis for designing more efficient antidotes against nerve agent intoxication.

Soman Inhibition of *Tc*AChE. It is well established that the P_SC_S stereoisomer of soman is the one that interacts preferentially with AChE.[25,28] Examination of the 3D structure of the nonaged soman/*Tc*AChE conjugate permits unequivocal assignment of the chirality of the covalently bound OP moiety. This is seen to be P_SC_R. The observation that the same absolute configuration (viz., P_S) is retained at the P atom in the nonaged adduct is attributed to stereoinversion at the P atom and to replacement of the fluoride leaving group by Ser200 Oγ, which has lower priority order than the fluorine atom in assignment of the absolute configuration (Scheme 2). Similar inversion and retention of the absolute configuration of the P atom was reported by Cygler et al.,[46] who determined the crystal structure of a lipase conjugated to a methyl hexylphosphonate transition state analogue. Stereoinversion at the P atom was also observed for the VX-*Tc*AChE adduct,[27] as well as for the VX/mAChE adduct;[47] however, in these cases, the P_R configuration was assigned because the $O-CH_2CH_3$ moiety has lower priority order than Ser 200 in determining the absolute configuration (Figure 4; Scheme 2). Recently, inversion of the configuration at the P atom was reported for reaction of tabun with mAChE and huBChE.[48] Thus, an in-line displacement is envisaged in all the cases reported for ChEs, regardless of the nature of the leaving group or the size of the O-alkyl substituent on the OP. This mode of nucleophilic attack is due to the steric constraints within the catalytic site that enforce the approach of the catalytic serine from the face opposite to the leaving group (Figure 4).

The P_S configuration of the soman/*Tc*AChE adduct was anticipated on the assumption that phosphonylation proceeds via an in-line displacement mechanism. However, the C_R stereochemistry of the pinacolyl Cα atom seen in the crystal structure is at odds with the kinetic measurements performed on various AChEs and BChEs, all of which slightly favor the P_SC_S diastereoisomer.[25,28] Two possible explanations may be provided: (a) Even though the P_SC_S isomer can be docked computationally into the active site without its distortion (not shown), steric constraints produced by crystal packing could change the chiral preference at Cα. (b) A second possibility is that inhibition of *Tc*AChE by the P_SC_S isomer is followed by a rapid rearrangement at the Cα atom, resulting from formation of a planar pinacolyl carbenium ion species that realkylates the oxygen of the OP moiety. This would preferentially generate the more stable P_SC_R adduct under the experimental conditions employed. Furthermore, we cannot rule out the possibility that *Tc*AChE preferentially selects the P_SC_R epimer. It would, therefore, be of interest, not only to compare the 3D crystal structures of soman/*Tc*AChE conjugates obtained from the individual P_SC_S and P_SC_R epimers but also to investigate the kinetics of their reaction with soluble *Tc*AChE. We note that similar rates of aging were observed for various AChEs inhibited with either the P_SC_R or the P_SC_S diastereoisomer.[13,18,25]

Comparison of the Inhibition of *Tc*AChE and of Human Carboxylesterase by Soman. It is of interest to compare the nonaged soman/*Tc*AChE crystal structure with that of the corresponding nonaged conjugate of human carboxylesterase 1 (huCE1; EC 3.1.1.1). It should be noted that the soman/huCE1 crystals were obtained by crystallization of the soman/huCE1 conjugate produced with soman (stereoisomeric mixture $P_{R/S}C_{R/S}$), which thus displayed no tendency to age over a period of 1−4 weeks,[49] as already reported for the rat CE1 conjugate.[50] huCE1 is a cholinesterase-like α/β hydrolase that contains a catalytic triad, an oxyanion hole, and a glutamate equivalent to Glu199. Figure 5 shows that all these residues can be superposed on the homologous residues in *Tc*AChE. However, the substrate specificity pockets in the two enzymes differ in size. Whereas the acyl-binding pocket in *Tc*AChE is too small to accommodate the bulky pinacolyl goup of soman, the analogous pocket in huCE1 is large enough to do so. In contrast, the pocket in huCE1 that is homologous to the large choline-binding pocket in *Tc*AChE is much smaller. Thus, the two enzymatic active sites bear a "mirror image" relation. This explains the difference in enantioselectivity between *Tc*AChE and huCE1 with respect to their reaction with soman. It was indeed recently shown that huCE1 reacts preferentially with the P_R isomer of soman in aqueous solution (Matthew Redinbo, personal communication), and it is the P_R configuration that is observed in the crystal structure of the soman/huCE1 conjugate.[49] This suggests that phosphonylation of huCE1 proceeds by a mechanism similar to the standard in-line displacement proposed for ChEs and lipases.[46]

Structural Comparison of the Nonaged Conjugates of AChEs with Soman, VX, and Tabun. Comparison of the crystal structure of the nonaged soman/*Tc*AChE conjugate with those of the nonaged VX/*Tc*AChE conjugate[27] and of the nonaged tabun/mAChE conjugate[48] reveals an interesting difference. In the VX/*Tc*AChE conjugate, there is a disruption of the catalytic triad, resulting in H440 Nε2

forming an H-bond with Glu199 instead of with Glu327, while in the tabun/mAChE conjugate, catalytic His447 and Phe338 shift in concert to avoid unfavorable contacts with the phosphoramidate group. In contrast, inhibition of *Tc*AChE by soman results in only a slight reorientation of the imidazole ring of His440 without disruption of the catalytic triad. A movement similar to that occurring upon phosphonylation with VX is precluded by the presence of the pinacolyl moiety, which is much more bulky than the ethoxy group of VX (Figure 4). Indeed, His440 Nε2 would be only 2.3 Å from the nearest methyl carbon of the pinacolyl moiety if it adopted the same conformation as in the nonaged VX/*Tc*AChE conjugate. The absence of a major conformational change of the catalytic histidine during aging of the soman/*Tc*AChE conjugate could explain partially its accelerated rate of aging relative to the VX/TcAChE conjugate. By contrast, in the nonaged tabun/huBChE conjugate, catalytic His438 is restrained by Phe398, a residue that is absent in the AChEs.[48]

Mechanism of Aging of the Soman/TcAChE Conjugate. The mechanism of aging (viz., dealkylation of the OP moiety) of conjugates of OP nerve agents with ChEs has been the topic of intense investigation and debate over the past 50 years. Aging of the soman/AChE conjugate has been a particular focus because its rapid rate presents a paramount toxicological challenge. The availability of a high-resolution crystal structure of the nonaged soman/*Tc*AChE conjugate, together with that of the homologous aged conjugate, at last permits a critical examination of the proposed mechanisms at the atomic level.

The proposed mechanisms were generated on the basis of kinetic data[51] and product analysis.[14] After the 3D structures of *Tc*AChE,[2] and subsequently of mAChE[52] and huAChE,[53] became available, dynamic modeling was attempted[19] and various mechanistic proposals were tested by site-directed mutagenesis.[19] On the basis of the pH-rate profile of aging[13,18] and the increased resistance of certain mutants to aging,[17,54] the following residues have been implicated in the aging of soman/AChE conjugates (*Tc*AChE numbering, with huAChE numbering in brackets): His440 (447), Trp84 (86), Glu199(202), Glu443(450), Phe331(338).[17,19,54]

Comparison of the crystal structures of the nonaged and aged soman/*Tc*AChE conjugates reveals a small, yet significant, movement of the imidazole ring of His440 (displacement of Nε2 by ~0.8 Å) that results in formation of a salt bridge with soman O2 in the aged conjugate (Figure 2C). In the case of the VX/*Tc*AChE conjugate, there is a much larger movement, which involves reformation of the catalytic triad and concomitant establishment of a salt bridge homologous to that seen in both the aged soman and aged sarin conjugates.[23] In the case of the tabun/mAChE conjugate, inspection of the crystal structure of the aged conjugate revealed a continuum of conformations that was ascribed, at least in part, to incomplete aging.[48]

The pH/rate profile of aging provides evidence that His440 is involved in the process. In the nonaged soman/*Tc*AChE conjugate, Nε2 of its imidazole ring is within H-bonding distance of both Ser 200 Oγ (2.7 Å) and O2 of the pinacolyl moiety (3.2 Å). The unfavorable bond angle for the H-bond with the pinacolyl O2, taken together with the restricted movement of the imidazole ring imposed by the bulky pinacolyl group, render it unlikely that His440 is directly involved in the aging process by protonation of O2. However, the proximity of the protonated Nε2 may confer a stabilizing electrostatic effect that could contribute to the observed pH-dependence.

Mutation of Glu199 (huAChE 202) to Gln slows the aging of soman-inhibited *Tc*AChE and huAChE to a similar extent.[17,19] In the electrostatic push−pull mechanism for dealkylation proposed by Viragh et al.,[13] Glu199 is proposed to play the "pusher" role, in conjunction with Trp84, triggering methyl migration from Cβ to Cα, with concomitant transformation of Cβ into a positively charged carbenium atom, resulting in Cα−O2 bond breakage. Because Cβ is near Trp84 in the crystal structure of nonaged soman/*Tc*AChE (4.6 Å; Figure 2A), the carbenium ion may indeed be stabilized by a cation−π interaction as proposed.[13] Once the carbenium ion is formed, it undergoes rapid rearrangement that could explain the composition of the low molecular weight products of "aging" as identified by Michel et al.[14] Because Glu199 is actually closer to Cα than to Cβ in the crystal structure, it seems unlikely that it would indeed play a "pushing" role. It may, however, stabilize the developing carbenium ion. Such an electrostatic stabilization is supported by the effect of mutagenesis of Glu199 to Gln (see above) and also by mutation of Glu443 (Glu450 in hAChE) to Ala; this latter residue is linked to Glu199 via a conserved water molecule (numbered 1002) and may thus be expected to stabilize its position.[2,42] Arguing against the push−pull mechanism as proposed by Viragh et al.[13] is the contention that methyl migration prior to carbenium ion formation would be most unfavored in energetic terms. We were unable to find an example in the literature in which methyl migration preceded carbenium ion formation. But methyl migration following carbenium ion formation is an accepted mechanism.[55] Indeed, in studies on the dealkylation of model OP compounds,[56] the composition of the observed olefin products was in line with the initial formation of a pinacolyl ion. The crystal structure of the nonaged conjugate described in the present paper provides a plausible mechanism for enhancement of carbenium ion formation as follows. The conserved water molecule 1001, which is hydrogen-bonded to Tyr121 Oζ, may enhance cleavage of the O2−Cα bond by increasing its polarity through hydrogen bonding to O2 (Figure 2A), while His440 would stabilize the partial charge on O2, thus releasing the unstable pinacolyl carbenium ion. This species immediately rearranges by methyl migration from Cβ to Cα to form the 2,3-dimethylbutyl carbenium ion that accounts for the principal olefin isolated. Trp84 may contribute to acceleration of dealkylation by stabilizing the developing positive charge on the pinacolyl moiety. In this context, it is interesting to note that the pinacolyl O2−Cα bond is elongated by 0.3 Å and thus weakened, if geometric restraints of this bond are down weighted in an alternate refinement of the nonaged soman/*Tc*AChE conjugate (see Supporting Information). The role of water 1001 in dealkylation could be checked experimentally by mutagenesis of Tyr121 (Tyr124 in huAChE). This mutation does not significantly affect the rate of phosphonylation,[57] but the aging rate of an OP conjugate of the mutant enzyme has not been compared to that of the corresponding conjugate of the wild-type enzyme.

In huAChE, mutation to Ala of Phe338 (Phe331 in *Tc*AChE) decreased the rate of aging of the soman conjugate by 160-fold,[19] whereas no effect was observed upon similar mutation of Phe337 (Phe330 in *Tc*AChE). Visual inspection of the 3D structure of the nonaged conjugate suggests that this mutation opens up a cavity into which the imidazole ring

of the catalytic His residue can move. This, in turn, could weaken the electrostatic stabilization of the developing carbocationic charge on the pinacolyl moiety.

Finally, it should be noted that the solvent-accessible volume of the gorge in the nonaged conjugate is decreased (6%) compared to the native structure. This decrease in gorge volume may generate a more suitably tuned vessel for catalyzing the dealkylation reaction by relevant enzyme residues. After dealkylation, a slight volume increase of 3% is observed but the volume of the gorge of the aged enzyme is still 3% less than that of the native form. Osmotic vs hydrostatic pressure, differential scanning calorimetry, and neutron scattering studies indicate that the thermodynamic stability of aged ChEs is strongly increased and that enzyme dynamics is altered compared to native enzymes.[58−60] Increased thermodynamic stability of aged ChEs was explained by dehydration at the bottom of the gorge so that the salt bridge between His440 and the phosphonyl moiety is in a low dielectric environment.

Nonfunctional Orientation of 2-PAM in the Ternary Complex with the Aged Soman/TcAChE Conjugate. The crystal structure of the ternary complex of 2-PAM with the aged soman/*Tc*AChE conjugate clearly reveals how 2-PAM binds within the CAS of the aged enzyme. The aromatic ring of 2-PAM stacks against the side chain of Trp84 in such a way that the oxime group points toward His440 O (the main-chain oxygen), at a distance of 2.5 Å; not only does it point away from the soman phosphorus atom, with its oxygen atom at a distance of 6.8 Å, but it is also on the wrong side for direct nucleophilic attack on the P-Ser200 Oγ bond. The orientation of 2-PAM differs from that seen in the complex of 2-PAM with native *Tc*AChE (Harel, Silman & Sussman, unpublished; PDB code 2VQ6). In this structure, too, the 2-PAM moiety is stacked against Trp84, but in a reversed orientation, so that its oxygen atom is 4.8 Å from Ser200 Oγ and could be substantially closer to the P atom in a putative OP conjugate.

Attempts were made to trap and solve the 3D structure of the ternary complex of 2-PAM with the nonaged soman/*Tc*AChE conjugate. To this end, crystallographic data were collected on a *Tc*AChE crystal that had been soaked for 5 min in a solution containing soman, at pH 8.2, followed by 5 min soaking in a 10 mM solution of 2-PAM at the same pH. No electron density was found that could account for the presence of 2-PAM, whereas the pinacolyl moiety of non-dealkylated soman was observed at the same position as in the nonaged soman/*Tc*AChE conjugate, viz., in proximity to Trp84, which would preclude binding of 2-PAM at that position as observed for the native enzyme and for the aged soman/*Tc*AChE conjugate (data not shown).

2-PAM thus binds poorly to the nonaged phosphonylated enzyme and binds in an unfavorable conformation after aging. Apart from 2-PAM, the oximes in use or under consideration for treatment of OP intoxication are elongated molecules and it was tacitly assumed that they span the active-site gorge, linking the PAS and the CAS, just like such potent bivalent AChE inhibitors as decamethonium[61,62] and heptylene-linked bistacrine.[63,64] Indeed, such an assumption was made in the design of an effective heptylene-linked bis-pyridinium aldoxime reactivator, Ortho-7.[65] However, the crystal structures of the complexes of three bis-quaternary oximes with mAChE, including Ortho-7,[66] provide strong evidence that their oximate groups attack OP/AChE conjugates from a position up the gorge axis, remote from the Trp residue in the CAS, and it is plausible that 2-PAM also acts on phosphylated conjugates from a similar angle and not as might be inferred from the crystal structures of the 2-PAM/*Tc*AChE complex or of its ternary complex with the aged soman/*Tc*AChE conjugate.

These findings should stimulate new approaches for improvement in the design of reactivators with better affinity for the nonaged conjugate or that could bind in the proper orientation after aging. Furthermore, because a nucleophilic attack is not prevented by the negative charge on the phosphonyl group,[67,68] reactivation of aged enzymes should in principle be made possible.

Template for Designing Novel Reactivators. A large number of putative reactivators have already been synthesized, some of which are currently being tested.[66,69] As already mentioned, they are mostly elongated molecules designed to bind simultaneously at the CAS and PAS of AChE. However, no molecule able to reactivate an aged OP/ChE conjugate has yet been found. Furthermore, there is scope for improving the potency of reactivators such as 2-PAM, HI-6, HLö-7, and MMB-4.

2-PAM, and its bisquaternary analogue, HI-6, are both 2-pyridinium monoaldoximes and yet, as mentioned above, display substantially different potencies in the reactivation of soman/AChE adducts.[70] Bimolecular rate constants of the reactivation for soman-inhibited AChEs by various oximes showed that in the case of human AChE HI-6 is 4×10^5-fold more potent than its monoquaternary parent analogue, 2-PAM. Furthermore, HI-6 was shown to reactivate the conjugate of mAChE obtained with the P_SC_S isomer significantly faster than that generated with the P_SC_R isomer[36] Similar results were reported for electric eel AChE inhibited with the same two potent soman epimers.[28] In this context, the crystal structure of the nonaged soman/*Tc*AChE conjugate presented here provides a valuable template for designing more potent reactivators. In particular, we propose to conduct molecular dynamics (MD) simulations of the nonaged soman/*Tc*AChE conjugate and take minor conformations accessed during the simulation into account in the design process. Indeed, a recent study showed that side chain conformations of gorge residues in crystallographic AChE−ligand complexes, which differ from those observed in native AChE, are already accessed in a MD simulation of native AChE.[71,72] Conformational changes upon ligand-binding in AChE thus involve pre-existing equilibrium dynamics, rather than an induced fit, and can be predicted to a certain extent. In the light of the considerations referred to above, it should also be of value to conduct docking experiments for 2-PAM and suitable bifunctional reactivators utilizing the crystal structures of native *Torpedo* and mammalian AChEs as well as of the nonaged and aged soman/*Tc*AChE conjugates.

Experimental Section

Materials. Polyethyleneglycol (PEG) 200 and morpholinoethylsulphonic acid (MES) were from Sigma Chemical Co. (St Louis, MO). *O*-(1,2,2-trimethylpropyl) methylphosphonofluoridate (soman) was obtained from the CEB (Centre d'Étude du Bouchet, Vert-le-Petit, France) and pralidoxime (*N*-methylpyridin-1-ium 2-aldoxime methiodide, 2-PAM) from EGA-Chemie (Steinheim, Germany). *Tc*AChE was purified as described previously.[2]

Crystallization and Soaking Procedures. Trigonal crystals of *Tc*AChE (space group $P3_121$) were obtained by the vapor diffusion

Table 1. Crystallographic and Refinement Statistics

	nonaged soman/TcAChE	aged soman/TcAChE	ternary 2-PAM/aged soman/TcAChE complex
PDB entry code	2wfz	2wg0	2wg1
ESRF beamline	ID14−4	ID14−2	ID14−2
temperature (K)	100	100	100
no. of frames	120	100	90
exposure time (s/frame)	1 (transmission 20%)	2	4
wavelength (Å)	0.939	0.933	0.933
space group	$P3_121$	$P3_121$	$P3_121$
unit cell parameters (Å)			
$a = b$	111.4	111.6	111.9
c	137.4	136.8	137.2
resolution range (Å)[a]	20.00−1.95 (2.00−1.95)	20.00−2.20 (2.30−2.20)	20.00−2.20 (2.30−2.20)
completeness (%)[a]	99.3 (98.8)	99.4 (99.9)	99.5 (99.4)
R_{sym} (%)[a,b]	7.3 (59.8)	13.7 (48.8)	8.0 (49.5)
$I/\sigma(I)$[a]	17.64 (3.12)	10.02 (3.25)	16.12 (3.30)
unique reflections[a]	71726 (5103)	50212 (6216)	50657 (6244)
redundancy	7.1	5.6	5.5
R_{cryst} (%)	16.62	17.72	16.58
R_{free} (%)	19.56	22.89	21.18
rmsd bond length (Å)	0.012	0.014	0.013
rmsd bond angles (deg)	1.3	1.5	1.4
no. of non-hydrogen atoms in ASU			
total	5206	5113	5221
protein	4395	4297	4449
water	660	620	555
ligands	151	196	217
carbohydrates	52	56	38
soman	10	4	4
2-PAM			10
B factor (Å^2)			
overall	31.4	25.4	31.2
protein	28.3	22.4	28.2
water	45.7	37.1	42.7
ligands	57.7	54.0	64.3
carbohydrates	61.2	56.6	64.6
soman	32.6	20.8	21.1
2-PAM			33.3

[a] Values in brackets refer to the highest resolution shell. [b] $R_{sym} = \frac{\sum_{hkl}\sum_{i}\left|I_i(hkl) - \overline{I(hkl)}\right|}{\sum_{hkl}\sum_{i} I_i(hkl)}$

method at 4 °C in hanging drops in 32−34% PEG 200 and 150 mM MES, at pH 5.8−6.1. Conjugates and complexes were formed by soaking crystals of the native enzyme at 4 °C into solutions based on either 36% PEG 200/150 mM MES, pH 5.8 (referred to as *soaking solution A*) or 36% PEG 200/150 mM Tris/HCl, pH 8.2 (referred to as *the soaking solution B*). To obtain the nonaged soman/*Tc*AChE conjugate, crystals were soaked for 6 min in *soaking solution B* containing 1.3 mM soman (mixture of the four stereoisomers $P_{R/S}C_{R/S}$). Because of the cryoprotective capacity of PEG 200 itself, no additional cryoprotectant was necessary and the crystal was directly loop-mounted and flash-cooled in liquid nitrogen. The aged soman/*Tc*AChE conjugate was obtained by soaking crystals for 2 h in *soaking solution A* containing 1.3 mM soman. Crystals of the ternary complex of the aged soman/*Tc*AChE conjugate with 2-PAM were obtained in two stages: first, crystals of the aged conjugate were obtained as described above; these crystals were then transferred for 12 h into *soaking solution A* or *B* containing 10 mM 2-PAM (solubilized initially at 100 mM in 150 mM Tris/HCl, pH 8). All soaking and flash-cooling operations were performed at the Centre de Recherches du Service de Santé des Armées (La Tronche).

Data Collection and Processing. All data collection was performed at the European Synchrotron Radiation Facility (ESRF, Grenoble) on beamlines ID14−2 and ID14−4. The loops containing flash-cooled crystals were transferred on the goniometer head into the cryostream of a cooling device (700 series, Oxford Cryosystems, Oxford, UK) operating at 100 K. For details concerning data collection, see Table 1. Reflections were indexed and integrated using XDS.[73] The intensities of integrated reflections were scaled using XSCALE, and structure factors were calculated using XDSCONV. Refinement of the models was carried out using Refmac5,[74] with the native structure of *Tc*AChE (PDB entry code 1EA5) as the starting model. For calculation of R_{free}, the same structure factors as the ones used for refinement of the starting model (1EA5) were flagged. For all three structures (viz., the nonaged soman/*Tc*AChE conjugate, the aged conjugate, and the ternary complex of the aged conjugate with 2-PAM), a rigid-body refinement was first carried out using reflections in the range of 20−4 Å. All model building and graphic operations were carried out using Coot.[75] In each model, the first set of water molecules was added automatically using the water-picking feature in Coot. Solvent molecules, ligands, and sugar residues of the covalently attached glycan chains, viz., *N*-acetylglucosamine (NAG) and fucose (FUC), were added subsequently. The occupancies of the soman adduct in the nonaged and in the aged conjugates were estimated to be 90% and 100%, respectively. 2-PAM and soman in the ternary complex were estimated to display full occupancy. Successive alternation of refinement cycles and manual model building were performed until R_{cryst} and R_{free} did not decrease any further. Refinement comprised energy minimization and individual isotropic B factor refinement, using the full range of recorded reflections for each data set. The simulated-annealing omit maps shown in Figures 2 and 3 were calculated using CNS

version 1.2[76] after omitting soman adducts and/or 2-PAM. Figures were produced with Pymol.[77] Active-site gorge volumes were calculated using the CASTP server[78] after removal of ligands and water molecules from the models. Alignment of huCE1 and *Tc*AChE structures was achieved with Theseus.[79] Final models were validated using MOLPROBITY[80] and WHATCHECK.[81] Parameters and topologies of PEG, MES, NAG, FUC, 2-PAM, and of nondealkylated and dealkylated soman adducts were generated using the PRODRG server at Dundee University.[82]

Acknowledgment. We gratefully acknowledge the ESRF for beam-time under long-term projects MX498, MX609, and MX722 (IBS BAG) and MX551 and MX666 (radiation-damage BAG), and the ESRF staff for providing efficient help during data collection. Financial support by the CEA, the CNRS, and the UJF is acknowledged, as well as a grant to M. W. from the Agence Nationale de la Recherche (ANR) (project no. JC05_45685), grants to F.N. from the ANR (ANR-06-BLAN-0163) and from the DGA (08co501), and a DGA grant (03co10-05/PEA 010807) to P.M. This study was supported by the European Commission Sixth Framework Research and Technological Development Program "SPINE2-COMPLEXES" Project, under contract no. 031220, a research grant from Erwin Pearl, the Benoziyo Center for Neurosciences, the Divadol Foundation, the Nalvyco Foundation, the Bruce Rosen Foundation, and the Neuman Foundation. J.L.S. is the Morton and Gladys Pickman Professor of Structural Biology. We thank Dr. Matthew Redinbo (Department of Chemistry, University of North Carolina at Chapel Hill) for permission to quote his unpublished data and Prof. David Milstein (Department of Organic Chemistry, Weizmann Institute of Science) for valuable discussions.

Supporting Information Available: Alternate refinement of the nonaged soman/*Tc*AChE conjugate. This material is available free of charge via the Internet at http://pubs.acs.org.

References

(1) Silman, I.; Sussman, J. L. Acetylcholinesterase: "Classical" and "Nonclassical" Functions and Pharmacology. *Curr. Opin. Pharmacol.* **2005**, *5*, 293–302.
(2) Sussman, J. L.; Harel, M.; Frolow, F.; Oefner, C.; Goldman, A.; Toker, L.; Silman, I. Atomic Structure of Acetylcholinesterase from *Torpedo californica*: A Prototypic Acetylcholine-Binding Protein. *Science*. **1991**, *253*, 872–879.
(3) Colletier, J. P.; Fournier, D.; Greenblatt, H. M.; Stojan, J.; Sussman, J. L.; Zaccai, G.; Silman, I.; Weik, M. Structural Insights into Substrate Traffic and Inhibition in Acetylcholinesterase. *EMBO J.* **2006**, *25*, 2746–2756.
(4) Harel, M.; Quinn, D. M.; Nair, H. K.; Silman, I.; Sussman, J. L. The X-Ray Structure of a Transition State Analog Complex Reveals the Molecular Origins of the Catalytic Power and Substrate Specificity of Acetylcholinesterase. *J. Am. Chem. Soc.* **1996**, *118*, 2340–2346.
(5) Rosenberry, T. L.; Johnson, J. L.; Cusack, B.; Thomas, J. L.; Emani, S.; Venkatasubban, K. S. Interactions between the Peripheral Site and the Acylation Site in Acetylcholinesterase. *Chem. Biol. Interact.* **2005**, *157*−*158*, 181–189.
(6) Bourne, Y.; Radic, Z.; Sulzenbacher, G.; Kim, E.; Taylor, P.; Marchot, P. Substrate and Product Trafficking through the Active Center Gorge of Acetylcholinesterase Analyzed by Crystallography and Equilibrium Binding. *J. Biol. Chem.* **2006**, *281*, 29256–29267.
(7) Eddleston, M.; Juszczak, E.; Buckley, N. A.; Senarathna, L.; Mohamed, F.; Dissanayake, W.; Hittarage, A.; Azher, S.; Jeganathan, K.; Jayamanne, S.; Sheriff, M. R.; Warrell, D. A. Multiple-Dose Activated Charcoal in Acute Self-Poisoning: A Randomised Controlled Trial. *Lancet* **2008**, *371*, 579–587.
(8) *Report of the Specialists Appointed by the Secretary-General to Investigate Allegations by the Islamic Republic of Iran Concerning the Use of Chemical Weapons*; no. S/16433 ; United Nations Security Council: New York, Mar 26, **1984**.
(9) *Report of the Mission Dispatched by the Secretary-General to Investigate Allegations of the Use of Chemical Weapons in the Conflict between the Islamic Republic of Iran and Iraq*; no. S/17911 ; United Nations Security Council: New York, Mar 12, **1986**.
(10) *Report of the Mission Dispatched by the Secretary-General to Investigate Allegations of the Use of Chemical Weapons in the Conflict between the Islamic Republic of Iran and Iraq*; United Nations Security Council: New York, May 8, **1987**.
(11) Macilwain, C. Study Proves Iraq Used Nerve Gas. *Nature* **1993**, *363*, 3.
(12) Nagao, M.; Takatori, T.; Matsuda, Y.; Nakajima, M.; Iwase, H.; Iwadate, K. Definitive Evidence for the Acute Sarin Poisoning Diagnosis in the Tokyo Subway. *Toxicol. Appl. Pharmacol.* **1997**, *144*, 198–203.
(13) Viragh, C.; Akhmetshin, R.; Kovach, I. M.; Broomfield, C. Unique Push−Pull Mechanism of Dealkylation in Soman-Inhibited Cholinesterases. *Biochemistry* **1997**, *36*, 8243–8252.
(14) Michel, H. O.; Hackley, B. E., Jr.; Berkowitz, L.; List, G.; Hackley, E. B.; Gillilan, W.; Pankau, M. Ageing and Dealkylation of Soman (Pinacolylmethylphosphonofluoridate)-Inactivated Eel Cholinesterase. *Arch. Biochem. Biophys.* **1967**, *121*, 29–34.
(15) Segall, Y.; Waysbort, D.; Barak, D.; Ariel, N.; Doctor, B. P.; Grunwald, J.; Ashani, Y. Direct Observation and Elucidation of the Structures of Aged and Nonaged Phosphorylated Cholinesterases by ^{31}P NMR Spectroscopy. *Biochemistry* **1993**, *32*, 13441–13450.
(16) Wins, P.; Wilson, I. B. The Inhibition of Acetylcholinesterase by Organophosphorus Compounds Containing a P−Cl Bond. *Biochim. Biophys. Acta* **1974**, *334*, 137–145.
(17) Saxena, A.; Doctor, B. P.; Maxwell, D. M.; Lenz, D. E.; Radic, Z.; Taylor, P. The Role of Glutamate-199 in the Aging of Cholinesterase. *Biochem. Biophys. Res. Commun.* **1993**, *197*, 343–349.
(18) Saxena, A.; Viragh, C.; Frazier, D. S.; Kovach, I. M.; Maxwell, D. M.; Lockridge, O.; Doctor, B. P. The pH Dependence of Dealkylation in Soman-Inhibited Cholinesterases and Their Mutants: Further Evidence for a Push−Pull Mechanism. *Biochemistry* **1998**, *37*, 15086–15096.
(19) Shafferman, A.; Ordentlich, A.; Barak, D.; Stein, D.; Ariel, N.; Velan, B. Aging of Phosphylated Human Acetylcholinesterase: Catalytic Processes Mediated by Aromatic and Polar Residues of the Active Centre. *Biochem. J.* **1996**, *318* (Pt 3), 833–840.
(20) Kovach, I. M. Stereochemistry and Secondary Reactions in the Irreversible Inhibition of Serine Hydrolases by Organophosphorus Compounds. *J. Phys. Org. Chem.* **2004**, *17*, 602–614.
(21) Ashani, Y.; Green, B. S. Are the Organophosphorus Inhibitors of AChE Transition State Analogs? In *Chemical Approaches to Understanding Enzyme Catalysis: Biometric Chemistry and Transition-State Analogs*; Green, B. S., Ashani, Y., Chipman, D., Eds.; Elsevier Scientific: Amsterdam, 1982; pp 169−188.
(22) Bencsura, A.; Enyedy, I.; Kovach, I. M. Origins and Diversity of the Aging Reaction in Phosphonate Adducts of Serine Hydrolase Enzymes: What Characteristics of the Active Site Do They Probe?. *Biochemistry* **1995**, *34*, 8989–8999.
(23) Millard, C. B.; Kryger, G.; Ordentlich, A.; Greenblatt, H. M.; Harel, M.; Raves, M. L.; Segall, Y.; Barak, D.; Shafferman, A.; Silman, I.; Sussman, J. L. Crystal Structures of Aged Phosphonylated Acetylcholinesterase: Nerve Agent Reaction Products at the Atomic Level. *Biochemistry* **1999**, *38*, 7032–7039.
(24) Benschop, H. P.; De Jong, L. P. A. Nerve Agent Stereoisomers: Analysis, Isolation and Toxicology. *Acc. Chem. Res.* **1988**, *21*, 368–374.
(25) Ordentlich, A.; Barak, D.; Kronman, C.; Benschop, H. P.; De Jong, L. P.; Ariel, N.; Barak, R.; Segall, Y.; Velan, B.; Shafferman, A. Exploring the Active Center of Human Acetylcholinesterase with Stereomers of an Organophosphorus Inhibitor with Two Chiral Centers. *Biochemistry* **1999**, *38*, 3055–3066.
(26) Berman, H. A.; Decker, M. M. Chiral Nature of Covalent Methylphosphonyl Conjugates of Acetylcholinesterase. *J. Biol. Chem.* **1989**, *264*, 3951–3956.
(27) Millard, C. B.; Koelnner, G.; Ordentlich, A.; Shafferman, A.; Silman, I.; Sussman, J. L. Reaction Products of Acetylcholinesterase and VX Reveal a Mobile Histidine in the Catalytic Triad. *J. Am. Chem. Soc.* **1999**, *121*, 9883–9884.
(28) Benschop, H. P.; Konings, C. A.; Van Genderen, J.; De Jong, L. P. Isolation, Anticholinesterase Properties, and Acute Toxicity in Mice of the Four Stereoisomers of the Nerve Agent Soman. *Toxicol. Appl. Pharmacol.* **1984**, *72*, 61–74.
(29) Millard, C. B.; Lockridge, O.; Broomfield, C. A. Organophosphorus Acid Anhydride Hydrolase Activity in Human Butyrylcholinesterase: Synergy Results in a Somanase. *Biochemistry* **1998**, *37*, 237–247.

(30) Wilson, I. B.; Ginsburg, S. Reactivation of Acetylcholinesterase Inhibited by Alkylphosphates. *Arch. Biochem.* **1955**, *54*, 569–571.
(31) Kewitz, H.; Wilson, I. B. A Specific Antidote against Lethal Alkylphosphate Intoxication. *Arch. Biochem. Biophys.* **1956**, *60*, 261–263.
(32) Wilson, I. B.; Froede, H. C. The Design of Reactivators for Irreversibly Blocked Acetylcholinesterase. In *Drug Design, Vol. II*; Ariens, E. J., Ed.; Academic Press: New York, 1971; pp 213−229.
(33) Worek, F.; Szinicz, L.; Thiermann, H. Estimation of Oxime Efficacy in Nerve Agent Poisoning: A Kinetic Approach. *Chem. Biol. Interact.* **2005**, *157−158*, 349–352.
(34) Marrs, T. C. Organophosphate Poisoning. *Pharmacol. Ther.* **1993**, *58*, 51–66.
(35) Antonijevic, B.; Stojiljkovic, M. P. Unequal Efficacy of Pyridinium Oximes in Acute Organophosphate Poisoning. *Clin. Med. Res.* **2007**, *5*, 71–82.
(36) de Jong, L. P.; Wolring, G. Z. Aging and Stereospecific Reactivation of Mouse Erythrocyte and Brain Acetylcholinesterases Inhibited by Soman. *Biochem. Pharmacol.* **1985**, *34*, 142–145.
(37) Yang, G. Y.; Oh, K. A.; Park, N. J.; Jung, Y. S. New Oxime Reactivators Connected with $CH_2O(CH_2)NOCH_2$ Linker and Their Reactivation Potency for Organophosphorus Agents-Inhibited Acetylcholinesterase. *Bioorg. Med. Chem.* **2007**, *15*, 7704–7710.
(38) Worek, F.; Thiermann, H.; Szinicz, L.; Eyer, P. Kinetic Analysis of Interactions between Human Acetylcholinesterase, Structurally Different Organophosphorus Compounds and Oximes. *Biochem. Pharmacol.* **2004**, *68*, 2237–2248.
(39) Ashani, Y.; Bhattacharjee, A. K.; Leader, H.; Saxena, A.; Doctor, B. P. Inhibition of Cholinesterases with Cationic Phosphonyl Oximes Highlights Distinctive Properties of the Charged Pyridine Groups of Quaternary Oxime Reactivators. *Biochem. Pharmacol.* **2003**, *66*, 191–202.
(40) Herkenhoff, S.; Szinicz, L.; Rastogi, V. K.; Cheng, T. C.; DeFrank, J. J.; Worek, F. Effect of Organophosphorus Hydrolysing Enzymes on Obidoxime-Induced Reactivation of Organophosphate-Inhibited Human Acetylcholinesterase. *Arch. Toxicol.* **2004**, *78*, 338–343.
(41) Ekstrom, F.; Akfur, C.; Tunemalm, A. K.; Lundberg, S. Structural Changes of Phenylalanine 338 and Histidine 447 Revealed by the Crystal Structures of Tabun-Inhibited Murine Acetylcholinesterase. *Biochemistry* **2006**, *45*, 74–81.
(42) Koellner, G.; Kryger, G.; Millard, C. B.; Silman, I.; Sussman, J. L.; Steiner, T. Active-Site Gorge and Buried Water Molecules in Crystal Structures of Acetylcholinesterase from *Torpedo californica*. *J. Mol. Biol.* **2000**, *296*, 713–735.
(43) Klebe, G. The Foundations of Protein−Ligand Interaction. In Crystallography and Drug Design, Erice, Italy, May 29−June 8, 2008.
(44) Petsko, G. A.; Ringe, D. *Protein Structure and Function*; New Science: London; Sinauer Associates: Sunderland, MA; Blackwell Publishing: Oxford, 2004; p xxii, 195 pp.
(45) Wang, E. I.; Braid, P. E. Oxime Reactivation of Diethylphosphoryl Human Serum Cholinesterase. *J. Biol. Chem.* **1967**, *242*, 2683–2687.
(46) Cygler, M.; Grochulski, P.; Kazlauskas, R. J.; Schrag, J. D.; Bouthillier, F.; Rubin, B.; Serreqi, A. N.; Gupta, A. K. A Structural Basis for the Chiral Preferences of Lipases. *J. Am. Chem. Soc.* **1994**, *116*, 3180–3186.
(47) Hornberg, A.; Tunemalm, A. K.; Ekstrom, F. Crystal Structures of Acetylcholinesterase in Complex with Organophosphorus Compounds Suggest That the Acyl Pocket Modulates the Aging Reaction by Precluding the Formation of the Trigonal Bipyramidal Transition State. *Biochemistry* **2007**, *46*, 4815–4825.
(48) Carletti, E.; Li, H.; Li, B.; Ekstrom, F.; Nicolet, Y.; Loiodice, M.; Gillon, E.; Froment, M. T.; Lockridge, O.; Schopfer, L. M.; Masson, P.; Nachon, F. Aging of Cholinesterases Phosphylated by Tabun Proceeds through O-Dealkylation. *J. Am. Chem. Soc.* **2008**, *130*, 16011–16020.
(49) Fleming, C. D.; Edwards, C. C.; Kirby, S. D.; Maxwell, D. M.; Potter, P. M.; Cerasoli, D. M.; Redinbo, M. R. Crystal Structures of Human Carboxylesterase 1 in Covalent Complexes with the Chemical Warfare Agents Soman and Tabun. *Biochemistry* **2007**, *46*, 5063–5071.
(50) Maxwell, D. M.; Brecht, K. M. Carboxylesterase: Specificity and Spontaneous Reactivation of an Endogenous Scavenger for Organophosphorus Compounds. *J Appl Toxicol.* **2001**, *21* (Suppl 1), S103–S107.
(51) Keijer, J. H.; Wolring, G. Z. Stereospecific Aging of Phosphonylated Cholinesterases. *Biochim. Biophys. Acta* **1969**, *185*, 465–468.
(52) Bourne, Y.; Taylor, P.; Marchot, P. Acetylcholinesterase Inhibition by Fasciculin: Crystal Structure of the Complex. *Cell* **1995**, *83*, 503–512.
(53) Kryger, G.; Harel, M.; Giles, K.; Toker, L.; Velan, B.; Lazar, A.; Kronman, C.; Barak, D.; Ariel, N.; Shafferman, A.; Silman, I.; Sussman, J. L. Structures of Recombinant Native and E202Q Mutant Human Acetylcholinesterase Complexed with the Snake-Venom Toxin Fasciculin-II. *Acta Crystallogr., Sect. D: Biol. Crystallogr.* **2000**, *56*, 1385–1394.
(54) Ordentlich, A.; Kronman, C.; Barak, D.; Stein, D.; Ariel, N.; Marcus, D.; Velan, B.; Shafferman, A. Engineering Resistance to "Aging" of Phosphylated Human Acetylcholinesterase. Role of Hydrogen Bond Network in the Active Center. *FEBS Lett.* **1993**, *334*, 215–220.
(55) Anslyn, E. V.; Dougherty, D. A. *Modern Physical Organic Chemistry*; University Science: Sausalito, CA, 2006; p xxviii, 1095.
(56) Cadogan, J. I. G.; Eastlick, D.; Hampson, F.; Mackie, R. K. Reactivity of Organophosphorus Compounds. Part XXIV. Acidic Hydrolysis of Dialkyl Methylphosphonates. *J. Chem. Soc. B* **1969**, 144–146.
(57) Kaplan, D.; Ordentlich, A.; Barak, D.; Ariel, N.; Kronman, C.; Velan, B.; Shafferman, A. Does "Butyrylization" Of Acetylcholinesterase through Substitution of the Six Divergent Aromatic Amino Acids in the Active Center Gorge Generate an Enzyme Mimic of Butyrylcholinesterase?. *Biochemistry* **2001**, *40*, 7433–7445.
(58) Gabel, F.; Masson, P.; Froment, M. T.; Doctor, B. P.; Saxena, A.; Silman, I.; Zaccai, G.; Weik, M. Direct Correlation between Molecular Dynamics and Enzymatic Stability: A Comparative Neutron Scattering Study of Native Human Butyrylcholinesterase and its "Aged" Soman Conjugate. *Biophys. J.* **2009**, *96*, 1489–1494.
(59) Masson, P.; Clery, C.; Guerra, P.; Redslob, A.; Albaret, C.; Fortier, P. L. Hydration Change During the Aging of Phosphorylated Human Butyrylcholinesterase: Importance of Residues Aspartate-70 and Glutamate-197 in the Water Network as Probed by Hydrostatic and Osmotic Pressures. *Biochem. J.* **1999**, *343*, 361–369.
(60) Masson, P.; Gouet, P.; Clery, C. Pressure and Propylene Carbonate Denaturation of Native And "Aged" Phosphorylated Cholinesterase. *J. Mol. Biol.* **1994**, *238*, 466–478.
(61) Felder, C. E.; Harel, M.; Silman, I.; Sussman, J. L. Structure of a Complex of the Potent and Specific Inhibitor BW284C51 with *Torpedo californica* Acetylcholinesterase. *Acta Crystallogr., Sect. D: Biol. Crystallogr.* **2002**, *58*, 1765–1771.
(62) Harel, M.; Schalk, I.; Ehret-Sabatier, L.; Bouet, F.; Goeldner, M.; Hirth, C.; Axelsen, P. H.; Silman, I.; Sussman, J. L. Quaternary Ligand Binding to Aromatic Residues in the Active-Site Gorge of Acetylcholinesterase. *Proc. Natl. Acad. Sci. U.S.A.* **1993**, *90*, 9031–9035.
(63) Colletier, J. P.; Sanson, B.; Nachon, F.; Gabellieri, E.; Fattorusso, C.; Campiani, G.; Weik, M. Conformational Flexibility in the Peripheral Site of *Torpedo californica* Acetylcholinesterase Revealed by the Complex Structure with a Bifunctional Inhibitor. *J. Am. Chem. Soc.* **2006**, *128*, 4526–4527.
(64) Rydberg, E. H.; Brumshtein, B.; Greenblatt, H. M.; Wong, D. M.; Shaya, D.; Williams, L. D.; Carlier, P. R.; Pang, Y. P.; Silman, I.; Sussman, J. L. Complexes of Alkylene-Linked Tacrine Dimers with *Torpedo californica* Acetylcholinesterase: Binding of Bis5-Tacrine Produces a Dramatic Rearrangement in the Active-Site Gorge. *J. Med. Chem.* **2006**, *49*, 5491–5500.
(65) Pang, Y. P.; Kollmeyer, T. M.; Hong, F.; Lee, J. C.; Hammond, P. I.; Haugabouk, S. P.; Brimijoin, S. Rational Design of Alkylene-Linked Bis-Pyridiniumaldoximes as Improved Acetylcholinesterase Reactivators. *Chem. Biol.* **2003**, *10*, 491–502.
(66) Ekstrom, F.; Pang, Y. P.; Boman, M.; Artursson, E.; Akfur, C.; Borjegren, S. Crystal Structures of Acetylcholinesterase in Complex with HI-6, Ortho-7 and Obidoxime: Structural Basis for Differences in the Ability to Reactivate Tabun Conjugates. *Biochem. Pharmacol.* **2006**, *72*, 597–607.
(67) Behrman, E. J.; Biallas, M. J.; Brass, H. J.; Edwards, J. O.; Isaks, M. Reactions of Phosphonic Acid Esters with Nucleophiles. I. Hydrolysis. *J. Org. Chem.* **1970**, *35*, 3063–3069.
(68) Behrman, E. J.; Biallas, M. J.; Brass, H. J.; Edwards, J. O.; Isaks, M. Reactions of Phosphonic Acid Esters with Nucleophiles. II. Survey of Nucleophiles Reacting with *p*-Nitrophenyl Methylphosphonate Anion. *J. Org. Chem.* **1970**, *35*, 3069–3075.
(69) Ekstrom, F. J.; Astot, C.; Pang, Y. P. Novel Nerve-Agent Antidote Design Based on Crystallographic and Mass Spectrometric Analyses of Tabun-Conjugated Acetylcholinesterase in Complex with Antidotes. *Clin. Pharmacol. Ther.* **2007**, *82*, 282–293.
(70) Luo, C.; Tong, M.; Chilukuri, N.; Brecht, K.; Maxwell, D. M.; Saxena, A. An in Vitro Comparative Study on the Reactivation of Nerve Agent-Inhibited Guinea Pig and Human Acetylcholinesterases by Oximes. *Biochemistry* **2007**, *46*, 11771–11779.

(71) Xu, Y.; Colletier, J. P.; Jiang, H.; Silman, I.; Sussman, J. L.; Weik, M. Induced-Fit or Preexisting Equilibrium Dynamics? Lessons from Protein Crystallography and MD Simulations on Acetylcholinesterase and Implications for Structure-Based Drug Design. *Protein Sci.* **2008**, *17*, 601–605.
(72) Xu, Y.; Colletier, J. P.; Weik, M.; Jiang, H.; Moult, J.; Silman, I.; Sussman, J. L. Flexibility of Aromatic Residues in the Active-Site Gorge of Acetylcholinesterase: X-Ray Versus Molecular Dynamics. *Biophys. J.* **2008**, *95*, 2500–2511.
(73) Kabsch, W. Automatic Processing of Rotation Diffraction Data from Crystals of Initially Unknown Symmetry and Cell Constants. *J. Appl. Crystallogr.* **1993**, *26*, 795–800.
(74) The CCP4 Suite: Programs for Protein Crystallography. *Acta Crystallogr., Sect. D: Biol. Crystallogr.* **1994**, *50*, 760-763.
(75) Emsley, P.; Cowtan, K. Coot: Model-Building Tools for Molecular Graphics. *Acta Crystallogr., Sect. D: Biol. Crystallogr.* **2004**, *60*, 2126–2132.
(76) Brunger, A. T. Version 1.2 of the Crystallography and NMR System. *Nat. Protoc.* **2007**, *2*, 2728–2733.
(77) DeLano, W. L. *The Pymol Molecular Graphics System*; DeLano Scientific: San Carlos, CA, 2002.
(78) Dundas, J.; Ouyang, Z.; Tseng, J.; Binkowski, A.; Turpaz, Y.; Liang, J. CASTp: Computed Atlas of Surface Topography of Proteins with Structural and Topographical Mapping of Functionally Annotated Residues. *Nucleic Acids Res.* **2006**, *34*, W116–W118.
(79) Theobald, D. L.; Wuttke, D. S. Theseus: Maximum Likelihood Superpositioning and Analysis of Macromolecular Structures. *Bioinformatics* **2006**, *22*, 2171–2172.
(80) Davis, I. W.; Leaver-Fay, A.; Chen, V. B.; Block, J. N.; Kapral, G. J.; Wang, X.; Murray, C L. W.; Arendall, W. B.III; Snoeyink, J.; Richardson, J. S.; Richardson, D. C. Molprobity: All-Atom Contacts and Structure Validation for Proteins and Nucleic Acids. *Nucleic Acids Res.* **2007**, *35*, W375–W383.
(81) Hooft, R. W.; Vriend, G.; Sander, C.; Abola, E. E. Errors in Protein Structures. *Nature* **1996**, *381*, 272.
(82) Schuttelkopf, A. W.; van Aalten, D. M.; PRODRG, A Tool for High-Throughput Crystallography of Protein−Ligand Complexes. *Acta Crystallogr., Sect. D: Biol. Crystallogr.* **2004**, *60*, 1355–1363.